Inventory of supplemental Information

Experimental procedures.
This section provides more detailed description of the experimental procedures used in the described studies.

Supplemental Figure S2
Is linked to Figure 2 in the main text.
This image shows electron micrographic analysis in Δ-prkar1a ß-cells, which show enlarged insulin vesicles, which are located closer to the cell membrane.

This finding directs attention of the findings made in vivo in the mouse model to the insulin secretory vesicle and vesicle exocytosis.

Supplemental Figure S3
Is linked to Figure 3 of the main text.
This image shows pharmacologic inhibition of cAMP-PKA signaling with Rp-8-CPT-cAMPs inhibited E4 action. These findings are complementary to those presented in Figure 3.

Supplemental Figure S4
Is associated to Figure 4 of the main text
This figure shows that specific pharmacologic PKA independent stimulation of EPAC2 stimulated EPAC2-SNAP25 interaction without affecting snapin phosphorylation. These findings are important to exclude a non PKA mediated pathway in the findings described related to snapin phosphorylation.

Supplemental Figure S5
Is associated to Figure 5&6 of the main text
This figure shows successful shRNA mediated specific snapin knockdown at mRNA and protein levels as well as successful re-expression of FLAG-tagged human snapin isoform overexpression. These studies provide important mechanistic complementary information to the studies presented in Figures 5 and 6.

Supplemental Table S1
This table is associated to Figure 1 of the main text and shows that PKA disinhibition in the pancreas does not change ß-cell proliferation or islet mass in mice.

Supplemental Table S2
This table is associated to Figure 2 of the main text and provides numerical data relevant to the graphs presented in figure 2.

Supplemental Table S3

This table is associated to Figure 3 of the main text and provides clinical information on human subjects with inactivating PRKAR1A mutations as well as on controls.

Supplemental Table S4
This table provides information on antibodies used in the studies presented in Figures 1-7

Supplemental material

Experimental procedures.

Animals

To generate DIO diabetic animals, 6-week old C57Bl/6J male mice were fed for 6 weeks a diet containing 60% calories as lipids (Bioserv). Controls were male littermates fed regular diet in parallel.

Glucose tolerance tests were performed by 2g/kg intraperitoneal (ipGTT) or gavage assisted oral (oGTT) introduction of 20% D-glucose followed by glucose measurements in tail vein blood at indicated intervals. Insulin tolerance tests were performed after intraperitoneal application of 0.5U/kg of recombinant human insulin (Novolin 100U/ml). For *in vivo* insulin secretion tests, serum insulin (Alpco) was measured in tail vein blood drawn after ip glucose administration. All dynamic tests in mice were performed after a 6 hour fast in three different litters at 8-9 weeks of age.

RT-PCR

Islet RNA was isolated using Illustra RNAspin combined with removal of DNA by DNAseI digestion (GE Healthcare). QPCR was carried out following standard procedures using SYBR green (BioRad) using mouse (FW: agctacagaactgtgccggatcaa, RV: gcttggagaaccaggagggtaaa) and Flag-tagged human snapin (FW: gccacagaactgtgccgcataaat, RV: cttatcgtcgtcatccttgtaatc) primers. All data was normalized to 36B4 housekeeping gene and quantitative measurements were obtained using the delta-delta CT method (Song et al., 2008). Human snapin expression was expressed relative to mouse snapin transcript in control (random shRNA) islets. Choice of primers allowed confirmation of mouse specific snapin knockdown and re-expression of human snapin isoforms in islets (**Figure S5AB)**.

Electron Microscopy

Pancreas tissues were dissected and for transmission electron microscopy (TEM) fixed in 3% glutaraldehyde (GA), 0.1 M Na cacodylate, 1% sucrose, 3mM $CaCl_2$ overnight at 4 °C. Samples were post-fixed in 1% OsO4 and 0.1 M sodium cacodylate, pH 7.4 followed by incubation in 2% uranyl acetate. After *en-bloc* staining, samples were ethanol dehydrated, passed through propylene epoxide, embedded in Eponate 12 (Ted Pella) and cured at 60 °C. Microtome cut sections (80 nm; Reichert Ultracut E) were placed on Formvar-coated copper grids and stained with uranyl acetate and lead citrate. Sections were viewed at 80 kV on a transmission electron microscope (H-7600; Hitachi) equipped with a dual CCD camera and digital software processor (Advanced Microscopy Techniques 1K.1K)

For immuno-electron microscopy (IEM) tissue was fixed in 4% paraformaldehyde/0.1 % GA, 0.1 M phosphate buffer (pH 7.4), 3% sucrose, 3 mM $MgCl_2$ at 4 °C followed by 0.12% tannic acid, 50 mM NH_4Cl and 2% uranyl acetate before preparing sections. For insulin immunodetection, sections were pretreated with 50 mM NH_4Cl followed by tris-buffered saline (TBS, pH 8.2), 1% bovine serum albumin, and incubated with guinea-pig anti insulin (1:1000, Linco), washed and incubated with 10 nm Protein A Gold 1:30 in TBS and then treated with 2% GA in 0.1M sodium cacodylate followed by 2% uranyl acetate.

Islet studies

Islets isolation, static insulin secretion and perifusion tests were performed as previously described (Chepurny et al., 2010; Hussain et al., 2006; Song et al., 2008) and initially incubated in 6 or 24-well culture plates in RPMI 1640 medium, 5 mM glucose supplemented with 10% FCS and 1% penicillin/streptomycin for 24 hours before performing additional procedures.

Insulin secretion during static incubation. After overnight culture (37 C, 5% CO2, 95% O2 in humid chamber) of isolated islets in RPMI 1640 (Mediatech) containing 5 mM glucose, 1% each Na-Pyruvate, HEPES, Penicillin/Streptomycin

and 2% bovine serum albumin (BSA), islets were switched to either low (3 mM) or high (10 mM) glucose containing RPMI 1640. Where indicated, E4 (10 nM) or 8-pCPT-2'-*O*-Me-cAMP-AM (EPAC selective stimulator, 10 μM) or vehicle (PBS or DMSO, respectively) was added. For inhibition studies, myristolated PKA Inhibitor (PKA specific inhibitor, myr-PKI 10 nM, Invitrogen), Rp-8-CPT-cAMPs (cAMP antagonist blocking PKA activation, 200 μM, Sigma) or vehicle (PBS) was added 20 minutes prior to adding E4. After 30 min incubation in low or high glucose concentrations, supernatant was taken for insulin measurements and pelleted islets were taken in acid ethanol (0.18M HCl in 70% ethanol) for insulin measurements in islets (ELISA, Alpco) or into protein lysis buffer for immunoblots (see below). Islet protein concentration was measured using (BCA method, Thermo Fisher)

Perifusion studies were performed as previously published (Chepurny et al., 2010; Hussain et al., 2006) with slight modifications. The perifusate was Krebs ringer buffer (KRB) (37 C, pH 7.4) containing 24 mM sodium bicarbonate and was gassed with 95% air and 5% CO2. Perifusion (1ml/min) occurred for the first 30 minutes with a KRB containing 3 mM glucose for equilibration, after which time the perifusate was collected in 1 ml fractions. After additional 10 minutes, glucose in the perifusate was increased to 10 mM. Where indicated, E4 (10 nM) and/or Rp-8-CPT-cAMPs (200 μM) was added to the perifusate. Insulin was measured in selected individual fractions of 3 mM and 10 mM glucose KRB perifusates (Ultrasensitive mouse insulin ELISA, Alpco). The first 10 minutes after increasing glucose was defined as first phase, the period thereafter was defined as second phase of insulin secretion. Insulin levels were normalized to total islet protein, which was spectrophotometrically determined (Eppendorf) after completion of the perifusion protocol.

Protein Co-immunoprecipitation

Immunoblots (IB) were performed with 40-50 μg protein taken in lysis buffer (Cell Signaling Technologies) Protein-protein interaction was assessed by co-

immunoprecipitation (Co-IP) studies (Co-immunoprecipitation (IP) followed by IB: Co-IP/IB). Briefly, approx 400-500 μg islet cell lysate was incubated in primary antibody at 4 °C overnight, before protein A agarose beads were added for 3 hours. Beads were washed in cell lysis buffer and resuspended in SDS sample buffer. For input control, 10% of total protein of respective source islet extracts were subjected to immunoblots in parallel. Actin was used as control for overall protein loading.

Human studies

For oGTT, data from subjects between less than 27 years of age were used in order to avoid any occult pituitary tumors or non-endocrine manifestations, which may confound the GTT. None of the subjects had a history of hypoglycemia or diabetes mellitus. All subjects had been previously bilaterally adrenalectomized and were clinically stable under substitution doses with glucocorticoid (cortisol) and –mineralocorticoid (fludrocortisone) treatment. No manifestations of endocrine hypersecretion was observed using clinical or laboratory tests at time of oral glucose tolerance tests. Patient characteristics are summarized in **Table S3.** During the oGTT, blood was drawn at indicated time points for glucose and insulin measurements (**Figure 3**).

Human islets were obtained from the Southern California Islet Resources Center and kindly accommodated by M. Shamblott (Kennedy Krieger Institute, Johns Hopkins University) with appropriate IRB approvals. Human islets were incubated in Functionality Media (Cellgro) with 1% human serum albumin for studies with E4 (10 nM in PBS; Sigma) stimulation. Islets were incubated in either E4 or vehicle only for 4 hours before protein extraction in RIPA buffer containing protease inhibitor cocktail and phosphate inhibitor III (Sigma Aldrich).

Supplemental Figure S2

Representative electron microscopic images of islets (**A, B**: 50000x magnification of transmission EM; **C, D** Immuno EM microscopy for insulin detection, 50000x magnification) of wt-prkar1a (top) and Δ-prkar1a (bottom) littermates. Δ-prkar1a islets exhibit increased vesicle size in proximity of intraislet capillaries, while dense cores containing insulin are unchanged. **Panels A and B** show capillaries (denoted by "c") with insulin vesicles along the capillary border (arrowheads).

E) Dense core size distribution in percent of total vesicles viewed. No difference between the various genotypes is observed (mean±SEM).

F) Size distribution of insulin vesicles within 1000 nm of capillaries in percent of total vesicles observed. Δ-prkar1a exhibit significantly larger vesicles. (mean±SEM, * signifies $p<0.05$).

G) Number of insulin vesicles aligned along intra-islet capillary/10μm of plasma membrane length. Δ-prkar1a ß-cells show significantly more vesicles adjacent to capillaries (mean±SEM, * signifies $p<0.05$).

Supplemental Figure S3

A. Mouse islets were treated with vehicle (PBS), E4 (10 nM), Rp-8-CPT-cAMPs (Rp-cAMPs)(200 μM), or E4+Rp-cAMPs. IP with snapin followed by IB for phosphoserine at low (3 mM) and high (10 mM) glucose. E4 stimulates snapin phosphorylation independently of glucose levels. Rp-cAMP inhibits E4 induced snapin phosphorylation. Bottom: immunoblot for protein input at bottom is 10% of islet protein before IP/IB.

B. Rp-8-CPT-cAMPS, a cAMP antagonist, which blocks PKA, inhibits E4 potentiation of GSIS

Perifusion studies of C57Bl/6 mouse islets in low (3 mM) followed by high (10 mM) glucose concentrations. Islets were treated with either PBS (inverted triangle), E4 (10 nM) (upright triangle), or E4 + cAMP antagonist Rp-8-CPT-cAMPS (200 μM) (circle) during perifusion. Table below curve summarizes area under the curves for first and second phase insulin secretion.*,#$p<0.05$ vs vehicle.

Supplemental Figure S4

Protein interaction between snapin and SNAP-25 or EPAC2, respectively, is stimulated by E4 in a PKA-dependent manner, whereas interaction between SNAP-25 and EPAC2 is stimulated in a PKA-independent (i.e. 8-pCPT-2'-*O*-Me-cAMP-AM) pathway.

Mouse islets were treated with vehicle (DMSO), 8-pCPT-2'-*O*-Me-cAMP-AM (8-C*O*P-cAMP) (10 μM), 8-C*O*M-cAMP (10 μM) + myr-PKI (10 nM), E4 (10 nM). Co-immunoprecipitation (IP/IB): Immunoprecipitation (IP) with snapin or SNAP-25 antibody, respectively, followed by immunoblot (IB) for interacting proteins SNAP-25 and EPAC2 was performed. Snapin interaction with SNAP-25 or EPAC2 occurs only with E4 stimulation and is inhibited by myr-PKI. SNAP-25 interaction with EPAC2 occurs with both E4 and 8-pCPT-2'-*O*-Me-cAMP-AM and is not inhibited by myr-PKI. Bottom: immunoblot for protein input at bottom is 10% of islet protein before IP/IB.

Supplemental Figure S5

Snapin knockdown in mouse islets and re-expression of FLAG-tagged human snapin isoforms. Isolated C57Bl/6 mouse islets were transduced with lentivirus expressing shRNA with mouse snapin specific sequences in conjunction with adenovirus transduction of FLAG-tagged human snapin WT, or S50A or S50D mutants

A: QPCR confirmation of endogenous mouse snapin knockdown by lentiviral snapin-specific shRNA, while scrambled shRNA remains inert.

B: QPCR confirmation of mRNA of FLAG-tagged human snapin isoforms after adeovirus mediated transduction

C: Immunoblot shows effective knockdown of snapin protein by shRNA and re-emergence of FLAG-tagged snapin after adenovirus transduction of FLAG – tagged human snapin isoforms. FLAG- specific immunoblot confirms expression of reintroduced snapin protein. SNAP25, collectrin, EPAC2 and VAMP2 protein levels are not affected by snapin shRNA knockdown.

D: Insulin secretion in static culture conditions. No effect is seen with E4 (10 nM) under low (3 mM) glucose conditions. At high (10 mM) glucose, re-expression of WT human snapin restores GSIS, while re-expression of S50A mutant has no effect. Re-expression of human snapin S50D results in augmented GSIS with no additional potentiation by E4.

Supplemental Tables

Supplemental Table S1

Pancreas morphometric parameters (islet area, ß-cells/islet, ß-cell size), proliferation indices (Ki67. Edu incorporation) and islet insulin content of genotype complements derived from pdx1-CRE/prkar1a $^{fl/fl}$ breeding. Data are from 8-9 months old animals. No significant differences are found between Δ-prkar1a mice and the other genotype complements. All parameters are given in mean±SEM; n=3 in each genotype group.

	wt-prkar1a	**het-prkar1a**	**Δ-prkar1a**
Parameter (Mean±SEM)			
Islet area ($\mu m^2 x10^3$)	14.26±0.76	14.38±0.81	14.5±0.80
ß-cell nuclei/islet	85.4±4.8	88.3±4.9	87.1±4.7
ß-cell size (μm^2)	169.1±2.1	163.6±2.1	166.4±0.7
Ki67+ ß-cells (% of all ß-cells)	3.5±0.12	3.6±0.26	3.4±0.15
EdU + ß-cells (% of all ß-cells)	4.6±0.20	5.3±0.33	5.9.±0.44
Islet insulin (ng/islet $x10^2$)	2.2±0.2	2.1±0.5	1.9±0.4

Supplemental Table S2

Area under the curves (AUC) during ip and oral glucose tolerance tests and insulin tolerance test in het-prkar1a, Δ–prkarıa and control littermate mice. Mean±SEM, * p<0.05 vs wt; # p<0.05 vs Δ–prkarıa.

ipGTT

AUC of glucose curves during ipGTT

	wt-prkar1a (n=13)	het-prkar1a (n=30)	Δ-prkar1a (n=14)
mg/dl*min			
Mean	21677	22321	11027*
SEM	869.4	723.2	359.7

AUC of insu10in curves during ipGTT

	wt-prkar1a (n=3)	het-prkar1a (n=3)	Δ-prkar1a (n=3)
ng/ml*min			
Mean	16.0	17.3	111.4*
SEM	5.32	3.07	12.88

AUC of glucose curves during ITT

	wt-prkar1a (n=13)	het-prkar1a (n=30)	Δ-prkar1a (n=14)
mg/dl*min			
Mean	3644	4032	3812
SEM	318.3	412.2	418.4

oGTT

AUC of glucose curves during oGTT

	wt-prkar1a (n=3)	het-prkar1a (n=3)	Δ-prkar1a (n=3)
mg/dl*min			
Mean	19970	14860*,#	11720*
SEM	474.2	646.0	353.0

AUC of insulin curves during oGTT

	wt-prkar1a (n=3)	het-prkar1a (n=3)	Δ-prkar1a (n=3)
ng/ml*min			
Mean	74.1	111.5*,#	164.2*
SEM	11.1	1.3	4.1

Supplemental Table S3

Patient characteristics

Patients with inactivating *PRKAR1A* mutation

Age	Sex	Height (cm)	Weight (kg)	Adrenalectomy	Medications
15	Female	158.4	96.4	2009	Hydrocortisone 15mg qam 5mg qpm Fludrocortisone 100 μg qam
17	Female	160.8	77.2	2009	Hydrocortisone 15mg qam 5mg qpm Fludrocortisone 100 μg qam
27	Female	162.9	57.9	1996	Hydrocortisone 20mg qam Fludrocortisone 100 μg qam
15	Female	156.7	51.6	2008	Hydrocortisone 15mg qam 5mg qpm Fludrocortisone 100 μg qam
17	Female	166.4	63.3	2003	Hydrocortisone 10mg qam 5mg qpm Fludrocortisone 150 μg qam
17	Female	159	61.9	2008	Hydrocortisone 15mg qam 5mg qpm Fludrocortisone 100 μg qam
17	Male	165.7	86.1	2008	Hydrocortisone 10mg qam 5mg qpm Fludrocortisone 100 μg qam

Patients with normal *PRKAR1A* gene sequence

Age	Sex	Height (cm)	Weight (kg)	Adrenalectomy	Medications
23	Male	156	60.8	2007	Hydrocortisone 10mg qam 5mg qpm Fludrocortisone 100 μg qam
12	Female	155.6	66.4	1994	Hydrocortisone 10mg qam 5mg qpm Fludrocortisone 100 μg qam
18	Female	164.5	60.1	1987	Hydrocortisone 17.5mg qam Fludrocortisone 100 μg qam
15	Female	na	40.9	2008	Hydrocortisone 10mg qam 5mg qpm Fludrocortisone 100 μg qam

Supplemental Table S4

Primary antibodies used for immunoblots and Immunohistochemistry.

Antibody	Vendor	Cat. No.	Dilution
Mouse anti Actin	Millipore	MAB1501	4000
Mouse anti PKA[RI]	BD Transduction Laboratories	610165	500
Mouse anti PKA[RIa]	BD Transduction Laboratories	610609	250
Mouse anti PKA[RIIa]	BD Transduction Laboratories	612242	2000
Mouse anti PKA[RIIB]	BD Transduction Laboratories	610625	2000
Mouse anti- PKA[C]	BD Transduction Laboratories	610980	2000
Rabbit anti CREB-1	Santa Cruz	sc-58	100
Rabbit anti Phospho S133 CREB	Abcam	ab30651	500
Rabbit anti Phosphoserine	Abcam	ab9332	100
Goat anti Snapin	Santa Cruz	sc-34946	100
Goat anti SNAP25	Santa Cruz	sc-7538	250
Rabbit anti- FLAG	Sigma-Aldrich	F7425	200
Rabbit anti- Collectrin	Santa Cruz	sc-135464	250
Rabbit anti- TRB-3	Santa Cruz	sc-67122	500
Mouse anti p27	Santa Cruz	sc-56338	200
Rabbit anti Cyclin A2	Abcam	ab7956-1	250
Rabbit anti Skp2p45	Santa Cruz	sc-7164	200
Rabbit anti Ser/thr O-GlcNAC	Gerald Hart, JHU	CTD110.6	500
Rabbit anti EPAC2	Santa Cruz	sc-25633	100
Mouse anti VAMP1/2	Santa Cruz	sc-58309	250
Guinea pig anti insulin	DAKO	A0564	1000
Rat anti Ki67	DAKO	M7249	10

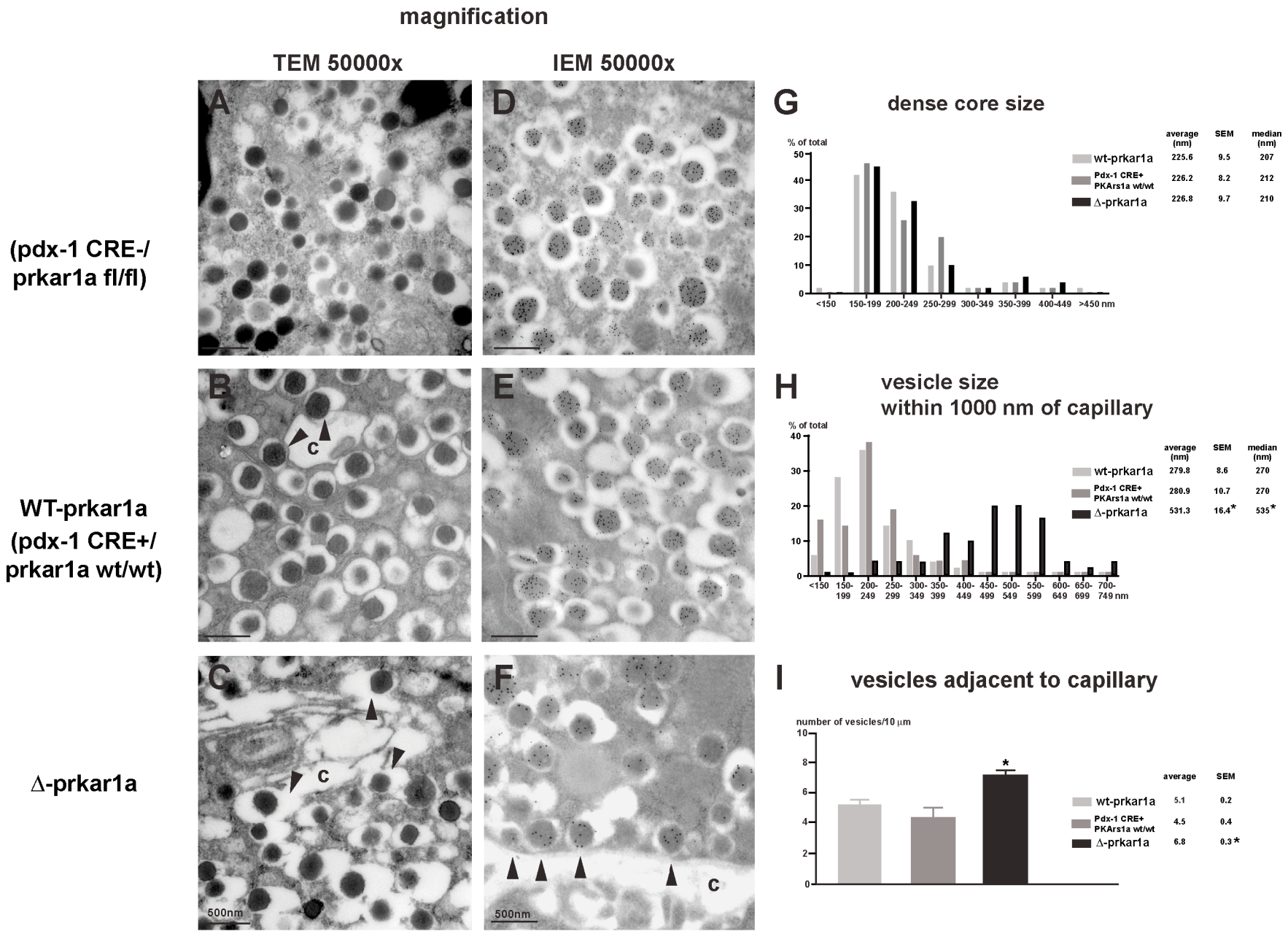
magnification
TEM 50000x
IEM 50000x
(pdx-1 CRE-/ prkar1a fl/fl)
WT-prkar1a (pdx-1 CRE+/ prkar1a wt/wt)
Δ-prkar1a
A
B
C
D
E
F
c
500nm
G
dense core size
% of total
average (nm)
SEM
median (nm)
wt-prkar1a 225.6 9.5 207
Pdx-1 CRE+ PKArs1a wt/wt 226.2 8.2 212
Δ-prkar1a 226.8 9.7 210
<150 150-199 200-249 250-299 300-349 350-399 400-449 >450 nm
H
vesicle size within 1000 nm of capillary
% of total
average (nm)
SEM
median (nm)
wt-prkar1a 279.8 8.6 270
Pdx-1 CRE+ PKArs1a wt/wt 280.9 10.7 270
Δ-prkar1a 531.3 16.4* 535*
<150 150-199 200-249 250-299 300-349 350-399 400-449 450-499 500-549 550-599 600-649 650-699 700-749 nm
I
vesicles adjacent to capillary
number of vesicles/10 μm
average
SEM
wt-prkar1a 5.1 0.2
Pdx-1 CRE+ PKArs1a wt/wt 4.5 0.4
Δ-prkar1a 6.8 0.3*

Supplemental Figure S3

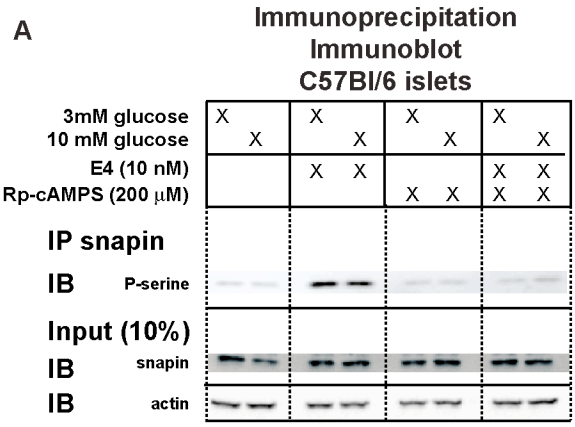

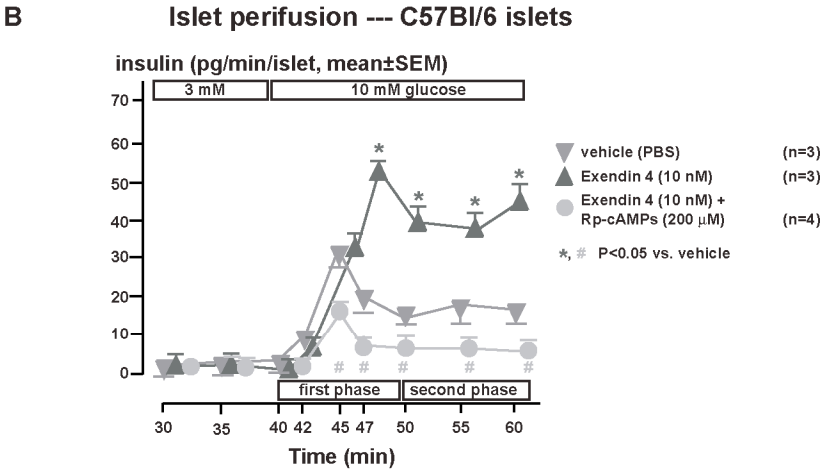

Area under the curve during perifusion (pg/islet, mean±SEM, *,#p<0/05 vs vehicle)	first phase	second phase
vehicle (PBS)	142.9±3.3	132.3±11.2
Exendin 4 (10 nM)	265.3±15.3*	373.4±31.2*
Exendin 4 (10 nM) Rp-cAMPs (200 μM)	90.0±7.5#	73.4±3.5.2#

Suppl Figure S4

Supplemental Figure S4

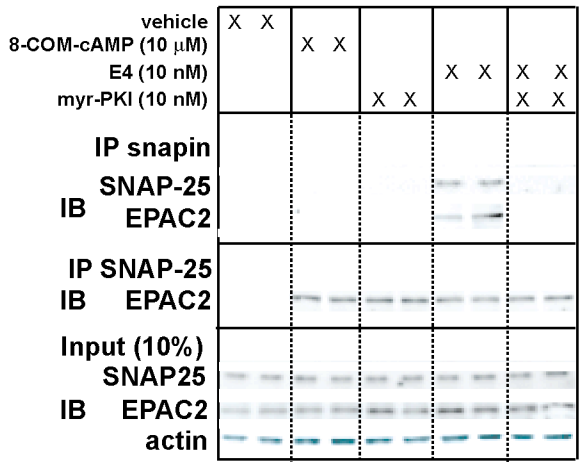

Suppl Figure S5

Supplemental Figure S5